Appl Nanosci (2015) 5:379–391
DOI 10.1007/s13204-014-0328-z

ORIGINAL ARTICLE

Hydraulic classifier system for fractionation of nano $CaCO_3$ particles

H. F. Aly · M. A. Akl · Hesham M. A. Soliman · Aref M. E. AbdEl-Rahman · A. I. Abd-Elhamid

Received: 28 April 2014 / Accepted: 5 June 2014 / Published online: 2 July 2014
© The Author(s) 2014. This article is published with open access at Springerlink.com

Abstract A laboratory scale hydraulic classifier system was developed for calcium carbonate nanoparticles fractionation. The system is based on the differences in the settling velocity of particles in aqueous fluid at different dynamic viscosities along different settling stages. Different factors affecting the fractionation process were studied, such as the effect of water volume, L, terminal (settling) velocity in different stages, v_s, $CaCO_3$ feed concentration, g/L and flow rate (L/h) of the dispersed fluid solution. The particles obtained were characterized using SEM and showed that the developed system can fractionate particles within the size range 25–33 nm. A simple model for the results obtained is developed and discussed in terms of the different parameters affecting particles size is given. Further, the calcium carbonate used was characterized before and after fractionations using Vibratory sieve shaker, SEM, EDS, XRD and FTIR.

Keywords Calcium carbonate · Nanoparticles · Fractionation · Hydraulic classifier

H. F. Aly
Hot Laboratories Center, Atomic Energy Authority, Nasr 13759, Egypt

M. A. Akl
Faculty of Science, Mansoura University, Mansoura, Egypt

H. M. A. Soliman · A. M. E. AbdEl-Rahman · A. I. Abd-Elhamid (✉)
Advanced Technology and New Materials Research Institute, City for Scientific Research and Technology Applications, P. O. Box 21934, SRTA, Egypt
e-mail: ahm_ch_ibr@yahoo.com

Introduction

Nanoparticles are now an important research area because they are widely used in numerous technological and medical applications (Guo et al. 2007). Owing to their very small size and large surface area-to volume ratio, fractionation of these powders is very attractive. Ultrafine powders can be obtained by mechanical attrition or by self-assembly using chemical reactions. In most cases, fractionation and classification of particles obtained are required.

Fractionation is one of the major techniques used for separation of nanoparticles. Many types of powder classifiers are available. These exemplified by cyclone type separators (Bryczkowski and Chmielniak 2001), cross flow air type classifiers (Wang et al. 2001), Rotating vibrating conical disk separator (Yamamoto et al. 1998) and impeller wheel type classifier (Galk et al. 1999). These classifiers address fractionation of powder particles within the micro range.

When concerning nanoparticles, a review on strategies for size and/or shape selective purification of nanoparticles was recently published by Kowalczyk et al. (2011). This review present and discuss different methods for separation of nanoparticles. Among these, methods based on the density gradient centrifugation are reported and discussed. In this system, particles are accelerated in a centrifugal field and particles of different sizes and/or shapes move with different velocities in the medium provided which is the basis for particles separation into distinct bands. To obtain selective separation between different particles sizes, the technique is modified by density gradient centrifugation in which a liquid column providing the density gradient required. This technique was successfully applied by Sun et al. (2009), to fractionate gold nanoparticles. The main advantages of these techniques are the speed and

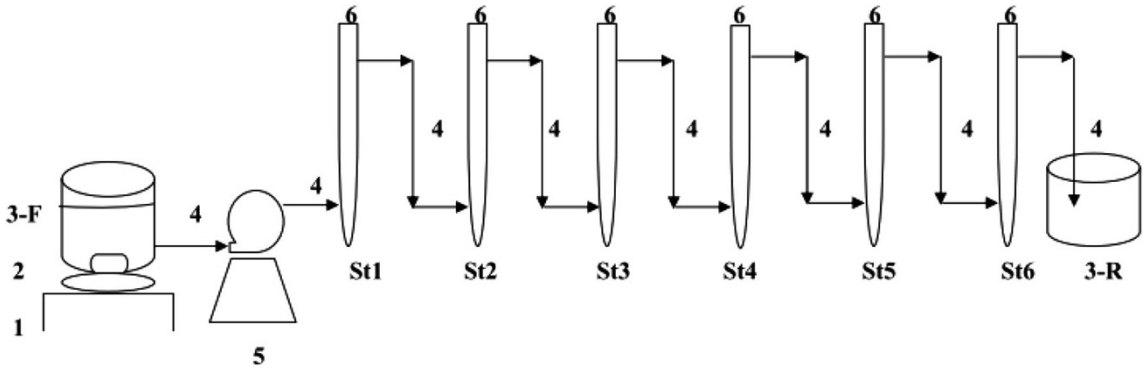

Fig. 1 Schematic diagram of hydraulic classifier system. 1) *magnetic stirrer*, 2) *Magnet*, 3-F & 3-R) *Glass beaker (2000 ml)*, 4) *plastic pipe*, 5) *Pump*, 6) *50 ml Plastic tubes*

selectivity of separation, provided that a suitable liquid is used to give the density gradient medium required without disturbing the nanoparticles to be fractionated.

In this contribution, a simple laboratory scale hydraulic classifier system was developed based on the kinetic gravity separation and settling velocity. The system is simple, economic (where we use one pump and water as fractionation medium), continuous and the particles obtained are homogenous and in the nanoscale. In this kind of separation, the particles are separated on the basis of differences in their terminal velocity (Van Kooy et al. 2004). The developed system was used for fractionation of calcium carbonate particles (commercial and artificial samples were used). However, the sample can be fractionated into different sizes at different settling stages. Further, a simple model for the results obtained is given.

Developed particles classifier system

Mechanical attrition is top-down approach for production of nanoparticles, in which milling was used, followed by particles fractionation and classification. In this concern, for particles classification to nanoparticles, a fractionation system was developed. This system is based on sorting particles by specific gravity in stream of hydraulic water that rises at a controlled rate. In this environment, heavier particles will settle down and discriminated while lighter particles will be carried out. This was followed for different stages to fractionate the different particles.

A schematic diagram for the system is given in Fig. 1. The system consists of 2L feed beaker, 3-F, contains the particles to be classified in certain volume of water. These fed particles are dispersed by a magnetic stirrer, 1, with a magnet, 2. After complete dispersion of the particles, the dispersed particles are feeding by a pump, 5, at constant flow rate, through a six stages test tubes (travelling zone),

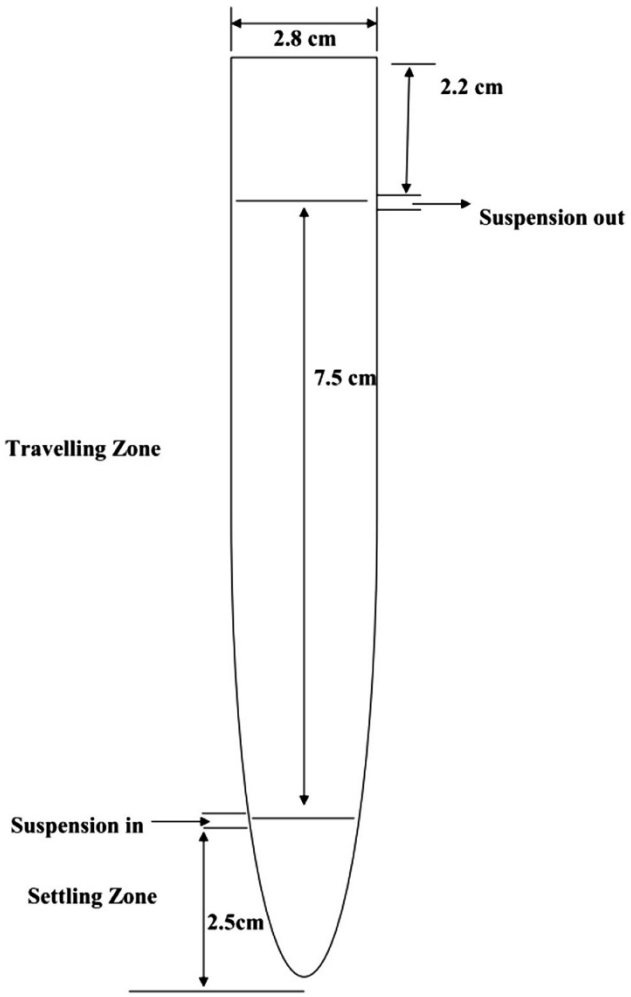

Fig. 2 Schematic diagram of the stage

connected in a series, from the top to the bottom of each tube. Based on the different factors affecting the flow rate of the suspended particles, which will be studied, the particles with different sizes will settle down in the cone part (settling zone) of the test tube of each stage. At the end of

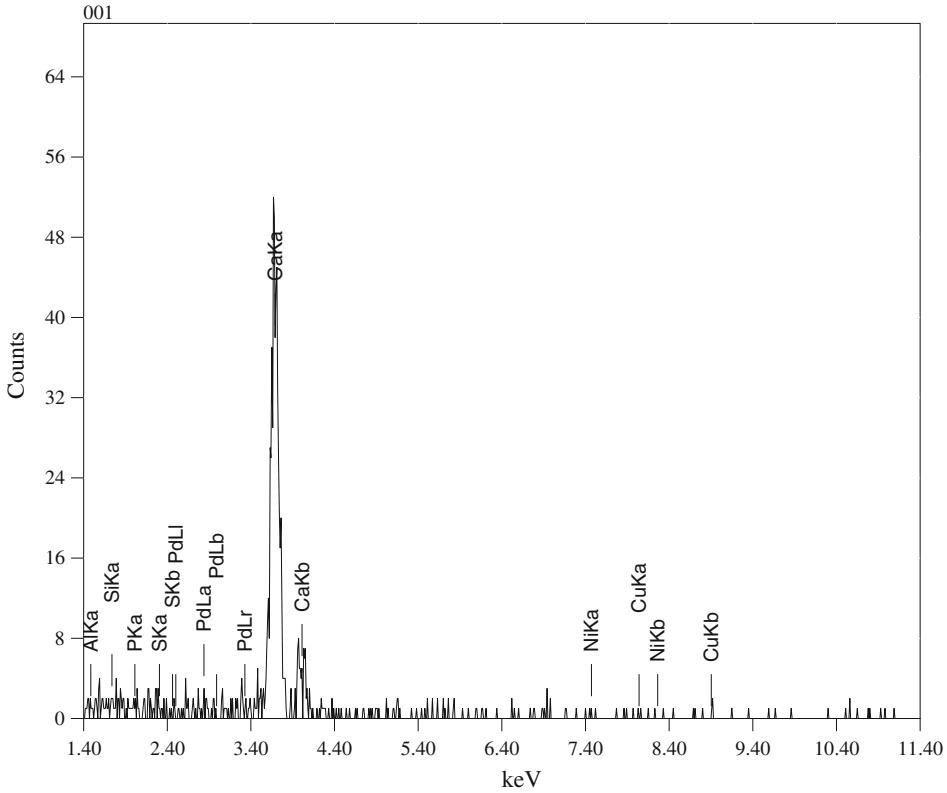

Fig. 3 The EDS analysis for calcium carbonate obtained from target for chemical industry company (S1)

Element	(keV)	mass%	Error%	At%	Compound	mass%	Cation K
C K	0.277	12.01	0.16	18.97			7.9586
O K	0.525	55.83	0.71	66.20			35.3681
Al K	1.486	0.01	0.24	0.01			0.0137
Si K	1.739	0.02	0.22	0.02			0.0286
P K	2.013	0.50	0.20	0.30			0.8193
S K	2.307	0.11	0.16	0.07			0.1956
Ca K	3.690	29.12	0.28	13.78			52.2119
Ni K	7.471	1.09	1.03	0.35			1.5658
Cu K	8.040	0.54	1.37	0.16			0.7427
Pd L	2.838	0.76	0.51	0.14			1.0958
Total		100.00		100.00			

the 6th test tube (St. 6), a receiving beaker, 3-R, is present to collect the end fraction of these particles. A detailed dimension of the tubes used at the different stages is given in Fig. 2. This system was used to fractionate two samples of commercial $CaCO_3$.

Experimental

Chemicals

Two samples of calcium carbonate were subjected to fractionation experiments. The first sample (S1) was obtained from Target Company for Chemical Industry, Alexandria, Egypt, its purity was determined by EDS analysis as seen in Fig. 3. In addition, the second one (S2) was obtained from Riedel–DeHaen Company, Germany (98.5 %).

Instruments

GP 3202 analytical balance (Sartorius, USA), SB 162 hot plate stirrer (Stuart, UK.) and Pump drive S101 (Heidolph, Germany).

AS200 Basic Vibratory Sieve Shaker (Retsch, Germany), JSM-636 OLA Scanning Electron Microscopy (SEM) (Jeol, Japan) with EDS analysis was used to measure the elemental analysis, XRD- 7000 X-Ray Diffraction (Shimadzu, USA), and 8,400 s Fourier transmission infra red spectroscopy (FTIR) Shimadzu, Japan.

Procedures

Sieving of $CaCO_3$

Two procedures were used in case of $CaCO_3$; dry sieving and wet sieving. In case of dry sieving, 100 g obtained from Target for chemical industry company, Alexandria, Egypt, or 5 g of $CaCO_3$ from Riedel-deHaën, Germany, was placed on vibratory sieve shaker for 10 min at amplitude of 100 mm. While in case of wet sieving, 5 g of $CaCO_3$ from (Target for chemical industry company, Egypt or Riedel-deHaën, Germany) was dispersed in 800 ml distill water for 2 h then poured on vibratory sieve shaker for 10 min at amplitude of 100 mm. The sieving for each size fraction was dried at 105 °C for 12 h.

Fractionation procedure

The fractionation procedure was carried out by taken a certain weight of $CaCO_3$ and well mixed in 800 ml of double distilled water using magnetic stirrer for a predetermined period. After stirring, the mixture was left for 10 min for settling of large particle size (< 20 μm). These particles were then separated from suspended particles by decantation and discarded. The separated dispersed particles were subjected to stirring and particle size fractionation by feeding at a predetermined flow rate into the hydraulic classifier apparatus developed in this work (Fig. 1). After a certain period enough to fractionate the particles in different stages, a drop of the settled particles separated in the bottom of the different fractionating stages was placed on a glass slide and subjected to air drying for SEM characterization. The different conditions affecting particle separation was applied on the sample S1 to obtain the optimum condition for particle classifications. The optimum condition for S1 sample was then applied to S2.

Particle size determination

To study the morphology of the particles present in samples, it was first coated with gold using Carbon Sputter Coater SPI, Module control, SPI supplies USA. When this surface is subjected to the electrons beam, the reflected beam of electrons carries a bright and clear image of it. After coating, the sample was placed in the cavity of JEOL JSM-6390 LA, Scanning Electron Microscope (SEM) provided with Smile View software for particle size measurements.

To obtain good statistical measurements for particle size, the work of Vigneau et al. (2000), was consulted. Accordingly, three drops from 6th stage sample was taken on three different slides. Each slide was scanned for at least 20 particles at different eight areas of the slide to give a total of 500 particles for the three slides (Fig. 4d). The particle size distribution for the three slides is shown in Fig. 3d. The mean particle size of the sample was found to equal 31 nm with standard deviation ±2 using the software Smile View.

Results and discussion

Sieving of $CaCO_3$

Two samples of different suppliers of calcium carbonate were studied as given in the experimental. A known weight of each sample was subjected to dry and wet sieving and the weight of each sieved fraction of certain particle size was determined. Tables 1 and 2 give the results of dry sieving, and Tables 3 and 4 are for wet sieving. These results indicated that wet sieving brought finer particles as well as better classifications. This is exemplified for both samples S1 and S2. In the case of sample S1, the largest particle size is in the range 250–125 μm for dry sieving whereby for the same sample, the largest particle size is 125–63 μm for wet sieving. Similar results were obtained for sample S2. For both samples, the smallest particle size was less than 45 μm. This fraction size was taken as feed source for further fractionation using the hydraulic system developed and given in this work.

Basic concept of the particles classifier

The main concept of this particle separator is based on the differences in the settling velocity of different particles in a fluid of different dynamic viscosities along the different stages. In this concern, the particles are transported from one stage to another leaving particle of terminal velocity at each stage.

The terminal velocity of sediment particles (negative velocity) is a defined as the rate at which the sediment settles in still fluid. This velocity is diagnostic of particle size and is also sensitive to the shape and density of particles as well as the viscosity and density of the fluid. All of these are integrated in the transport parameter from stage to another. To predict the particle settling velocities, the main forces acting on a particle in fluid are the particle weight, the particle buoyancy and the drag force of the fluid. The difference between the weight force, F_w, and the buoyancy force, F_b, is the net gravitational force, F_g, given by:

$$F_g = F_w - F_b$$

Since, $F_w = \rho_s.V\,g$

and $F_b = \rho_f.\,V\,g$

Then, $F_g = (\rho_s - \rho_f)\,V\,g$ where ρ_s and ρ_f are the particle and fluid densities, and V is the volume of sediment particles and g is the acceleration of gravity.

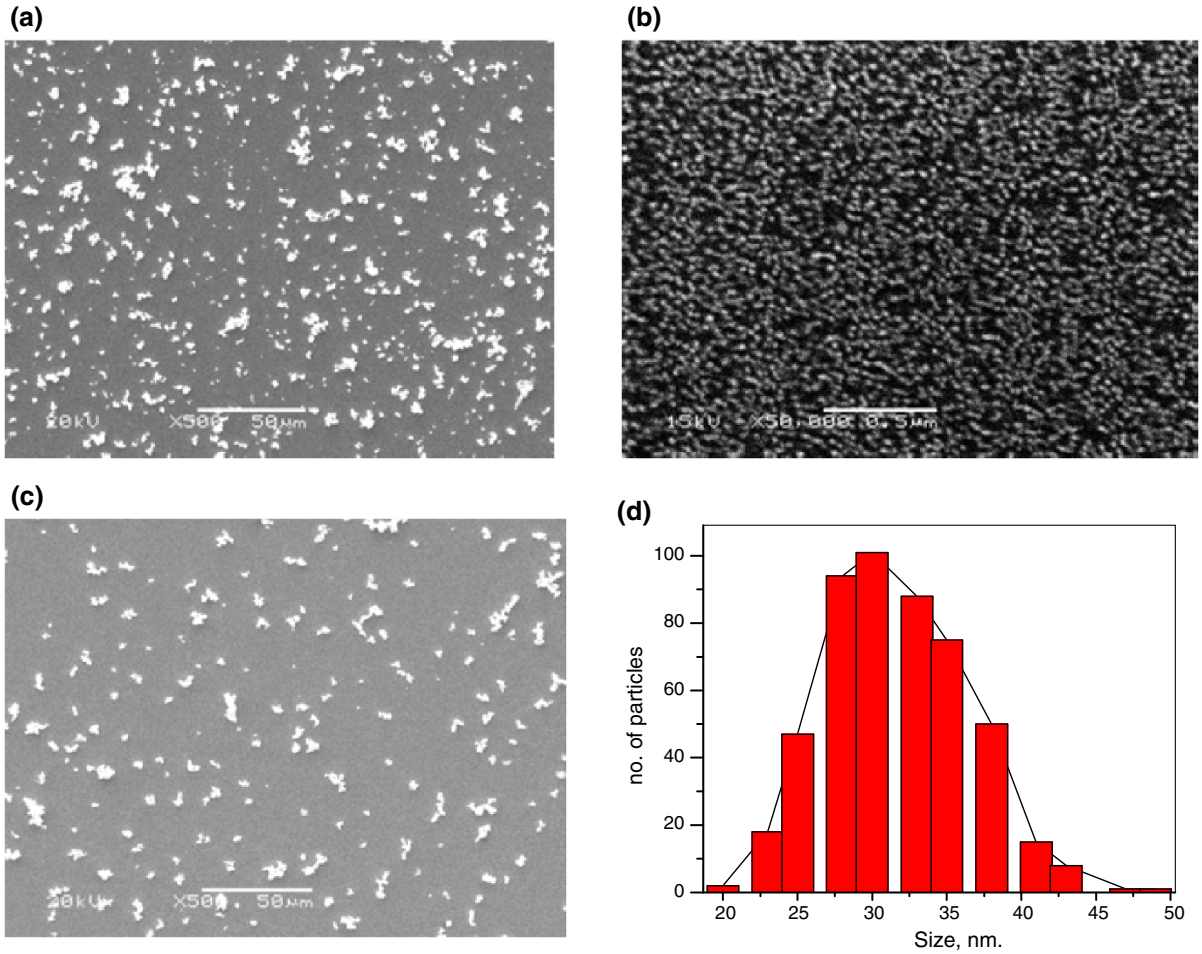

Fig. 4 Effect of water volume (L). 6th Stage, Stirring time: 2 h, Stirrer speed: 650 rpm, [$CaCO_3$]: 5g/800L, V_{water}. **a** 0.5 L, **b** 0.8 L and **c** 1.5 L

Table 1 Weight of different sizes of $CaCO_3$ (S1) after dry sieving

Size (μm)	Weight (g)
250–125	81.30
125–63	18.52
63–45	0.10
<45	0.05

$CaCO_3$ weight = 100 g, amplitude = 100 mm, time = 10 min

Table 2 Weight of different sizes of $CaCO_3$ (S2) after dry sieving

Size (μm)	Weight (g)
500–250	0.14
250–125	3.84
125–63	0.97
63–45	0.08
<45	0

$CaCO_3$ weight = 5 g, amplitude = 100 mm, time = 10 min

Table 3 Weight of different sizes of $CaCO_3$ (S1) after wet sieving

Size (μm)	Weight (g)
125–63	0.03
63–45	0.02
<45	4.2

$CaCO_3$ weight = 5 g, water volume = 800 ml, dispersing time = 2 h, sieving amplitude = 100 mm, sieving time = 10 min

Table 4 Weight of different sizes of $CaCO_3$ (S2) after wet sieving

Size (μm)	Weight (g)
250–125	0.06
125–63	0.05
63–45	0.03
<45	4.7

$CaCO_3$ weight = 5 g, water volume = 800 ml, dispersing time = 2 h, sieving amplitude = 100 mm, sieving time = 10 min

Assuming that the particles are spherical, then;

$$F_g = (\pi/6)\, d^3(\rho_s - \rho_f)\, g \quad (1)$$

where d is the diameter of the particles.

Equation 1 represents the net gravitational force on spherical particle. This force is downward (positive) if the sediment particles are denser than the fluid and upward (less than zero) if the sediment particles are less dense than the fluid.

Imagine a sediment spherical particle initially at rest, once the fluid transports the particles, velocities increase and the particles now moving through the fluid and get a fractional drag force, F_D. This drag force is dependent on the particles size and relative velocity, and the fluid viscosity (Stokes 1891).

The net force of the particle will be the differences between the net gravitational force and the drag force, and the particle will settle down once its velocity equals the settling velocity. This was given by the stocks law, which expresses the drag force in terms of the dynamic viscosity, μ, and the diameter of the particle, d, as well as the settling velocity, v_s, for small particles moving with laminar flow. This law is given by the following relation (Barry and Napier-Munn 2006; Rhods 2008);

$$F_D = 3\pi\, \mu\, v_s d \quad (2)$$

Under these conditions, $F_D = F_g$

Therefore, from Eqs. 1 and 2,

$$(\pi/6)\, d^3(\rho_s - \rho_f) g = 3\pi\, \mu\, v_s d$$

or,

$$v_s = \left(g d^2/18\mu\right)(\rho_s - \rho_f) \quad (3)$$

Equation 3, indicates that the settling velocity is indirectly proportional to the dynamic viscosity μ, as long as $(\rho_s - \rho_f)$ is constant, (http://www.gordonengland.co.uk/conversion/dynamic_viscosity.htm).

Experimentally, μ were calculated from flow rate/vertical travelled distance Kg s^{-1} $m^{-1}$and, at constant flow rate and feed concentration, v_s is directly proportional to $(\rho_s - \rho_f)$, and ρ_s was calculated from feed concentration in each stage/volume, kg m^{-3}, and ρ_f were calculated from feed concentration in each stage/volume, kg m^{-3}.

Further, the settling velocity is directly proportional to the square root of particle diameter at constant dynamic viscosity.

Factors affecting particles classification

Based on the basic concept of the developed fractionation system, the following factors affecting particle diameter, the following factors were investigated.

Effect of water volume (L)

Three different water volumes for the feed solution were used to show the effect of these volumes on the particle size of the $CaCO_3$, while keeping the other parameters constant. Figure 4a–c shows the size of the particles using 0.5, 0.8 and 1.5 L of water, respectively. It is clear that the particles size of average 25–33 nm is obtained when using 0.8 L of water, Figure 4b, while those obtained when using more or less of this volume (0.5 and 1.5 L)were of average size of 1.1–6.5 μm and 1.4–9 μm, Fig. 4a and c, respectively. These variations can be related to the fact that at low volume (500 ml water), the proportion of solids in water increases with subsequent increase in the pulp density and formation of particles aggregate. On the other hand at high dilution, 1,500 ml, the stirring efficiency decreases with subsequent decrease in separation efficiency. This result indicates that for feed concentration of 5 g $CaCO_3$ dispersed in 800 ml distilled water the different particles are well dispersed by the mixing speed used.

Effect of terminal (settling) velocity in different stages

The SEM images, Fig. 5, shows that the particles size range obtained at stages 3, 4, 5 and 6 are between 1.2 and 10.3 μm, Fig. 5a, 0.7–5.7 μm, Fig. 5b, 0.066–0.178 μm, Fig. 5c, and 30–47 nm, Fig. 5d, respectively. This indicates that as the number of stage increases, the size of particle decreases. Accordingly, particles of nano size, 30–47 nm, are separated in the 6th stage of classifier system.

To discuss the variations in the particles size obtained in each stage, equation, 3, was consulted. In this concern, the terminal (settling) velocity at a certain stage n will be given by the following relation:

$$v_{s,n} = (g/18) * \left[(\rho_s - \rho_f)_n / \mu_n\right] * d_n^2 \quad (4)$$

where n is the stage number at a certain stage, n $(\rho_s - \rho_f)_n$ and μ_n are constant. Then,

$$v_{s,n} = k_1 * d_{n,}^2 \quad \text{where } k_1 \text{ is constant} \quad (5)$$

Therefore, the relation between $v_{s,n}$ and d_n^2 will give linear relation, with negative slope, since $v_{s,n}$ is a downward velocity. The experimental results obtained are given in Fig. 6, and showed a linear negative relation with a slope equals –97 s. This support Eq. 6 deduced based on the previous assumptions.

Effect of $CaCO_3$ feed concentration (g/L)

The concentration of calcium carbonate in the feed dispersed solution was investigated in the range 1.5–15 g/800 ml. At all concentration used, the flow rate of the feed

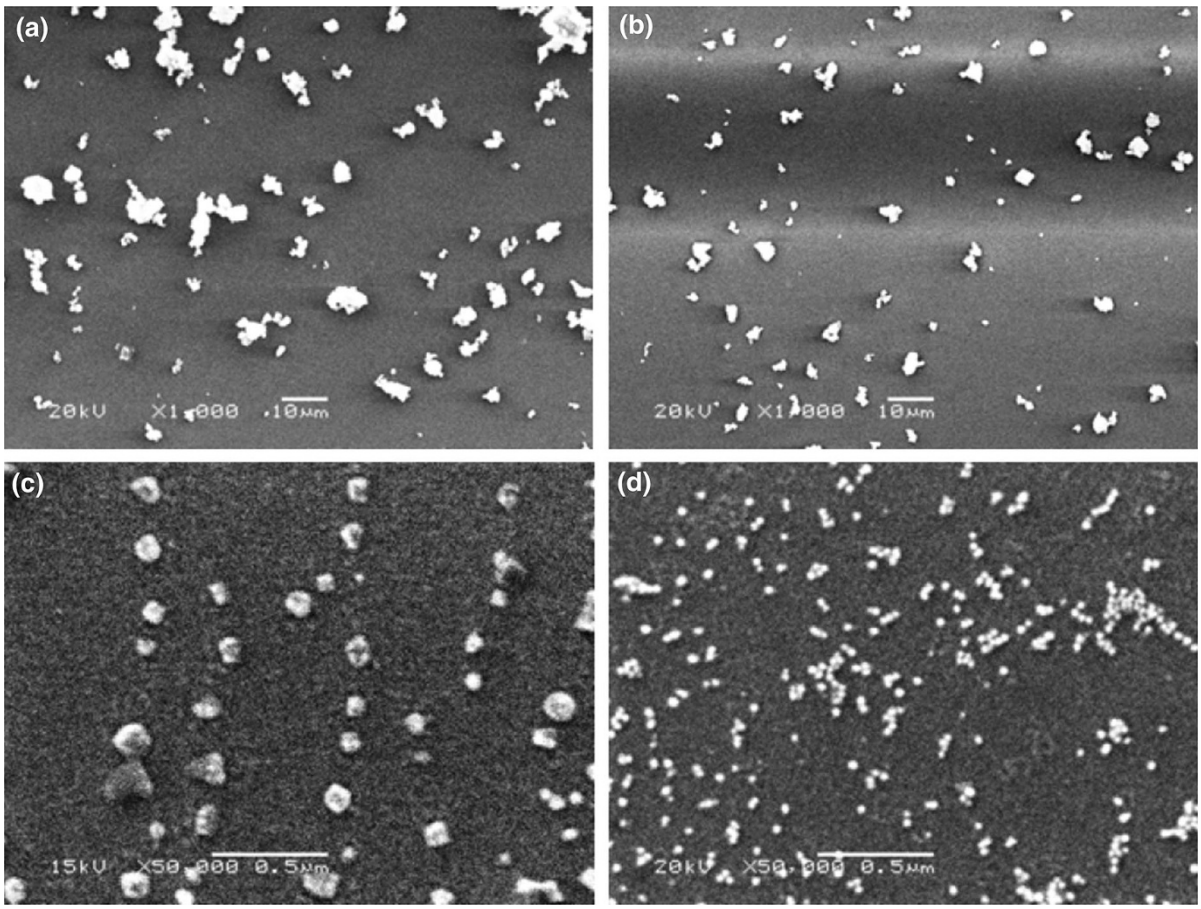

Fig. 5 Effect of terminal (settling) velocity in different stages. [$CaCO_3$]: 1.5g/800 L, Stirring time: 2 h, Stirrer speed: 650 rpm, Flow rate: 0.2 L/h. **a** 3rd stage, **b** 4th stage, **c** 5th stage and **d** 6th stage

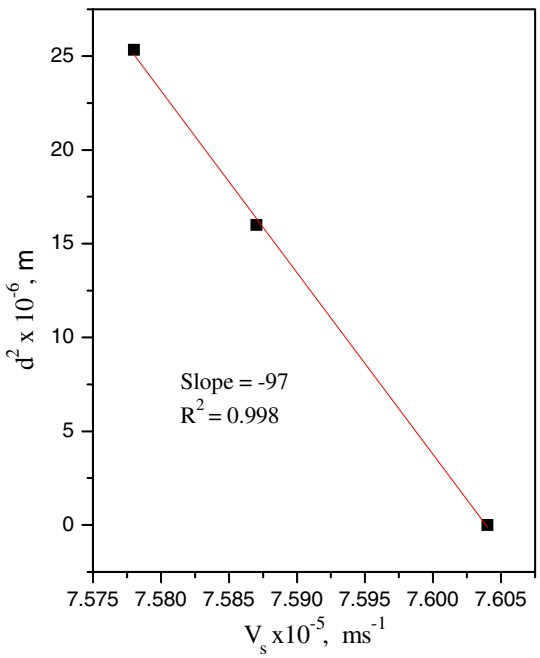

Fig. 6 Effect of the velocity of fluid on the particle size of $CaCO_3$ obtained at 6th stage

dispersed solution was 0.2 L/h, a mixing speed was 650 rpm and the stirring time was 2 h. The separated particles at 6th stage were determined for each feed concentration, Fig. 7a–d. When the feed of $CaCO_3$ concentration was 1.5 g/800 ml, the nanoparticles formed in the 6th stage obtained was in the range 30–47 nm (Fig. 7a). Increasing the concentration of the dispersed particles to 5 g/800 ml the range of the nanoparticles separated decreased to 25–33 nm (Fig. 7b). At higher dispersed $CaCO_3$ concentration, 10 and 15 g/800 ml, the $CaCO_3$ range of particle size obtained at 6th stage increased to 0.137–0.231 μm (Fig. 7c) and 0.156–0.429 μm (Fig. 7d), respectively. The impact of the dispersed phase concentration on particle classification is mainly related to the mechanical viscosity, μ, as long as no aggregate of particles are present in the dispersed phase.

Equation 3 can be modified to relate the particle diameter in terms of dynamic viscosity as follows:

$$d^2 = (18/g) * [v_s/(\rho_s - \rho_f)] * \mu \quad (6)$$

Then, the particle diameter at certain stage n will give the following relation:

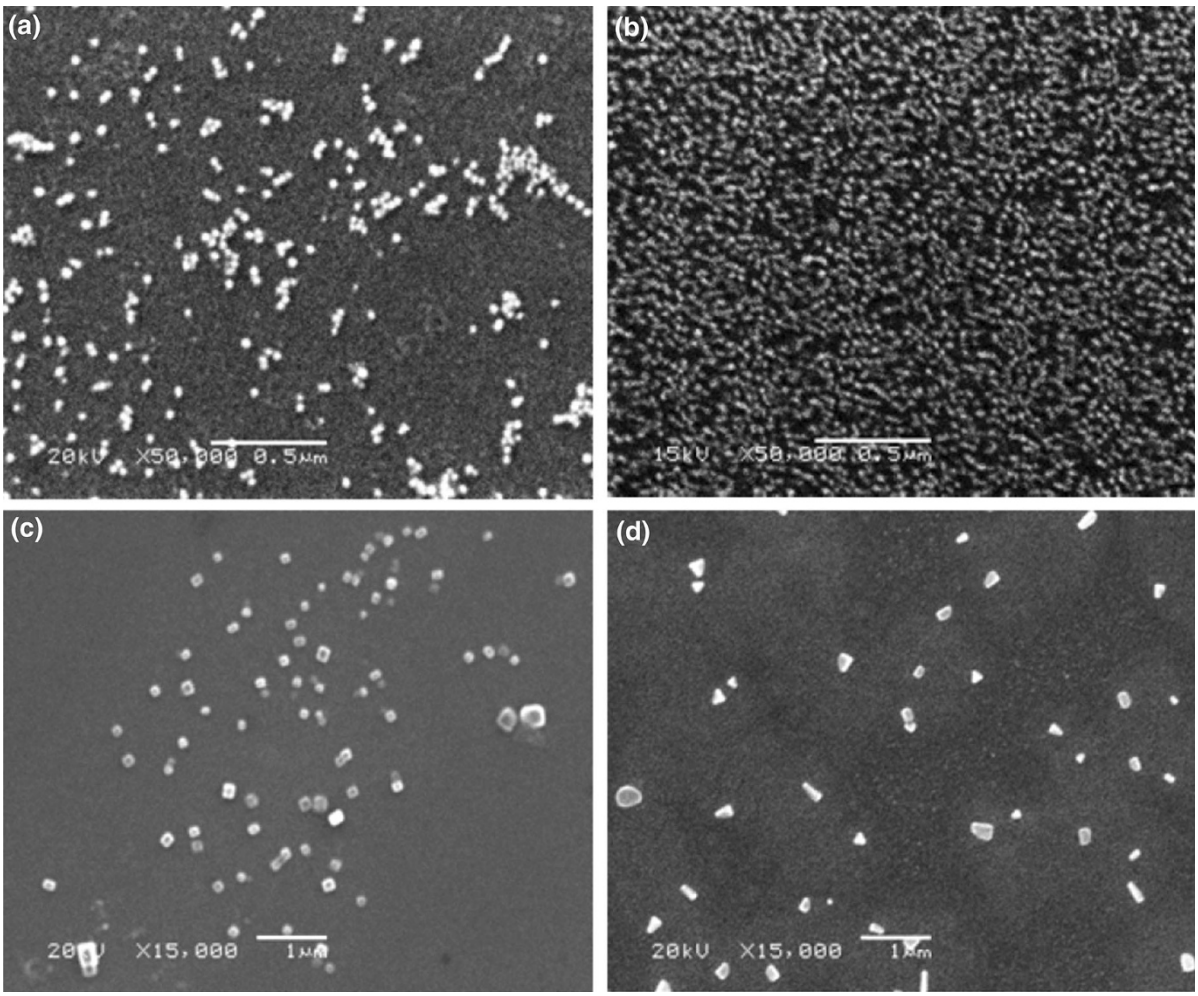

Fig. 7 Effect of $CaCO_3$ feed concentration on $CaCO_3$ particles size at 6th stage. Stirring time: 2 h. Stirrer speed: 650 rpm. Flow rate: 0.2 L/h. Water volume: 800 ml, wt_{CaCO_3} Wt_{CaCO3} **a** 1.5 g, **b** 5 g, **c** 10 g and **d** 15 g

$$d_n^2 = (18/g) * \left[v_{s,n}/(\rho_s - \rho_f)_n\right] * \mu_n \quad (7)$$

For certain concentration and stage $v_s/(\rho_s - \rho_f)$ is constant.

$$\text{Then, } d_n^2 = k_2 * \mu_n \quad (8)$$

Figure 8 shows a linear relation between d_n^2 and μ_n with positive slope 0.22 m^2 s kg^{-1} was obtained. This indicates that the particle diameter is directly proportional to the viscosity of the fluid at certain stage and this support Eq. 8.

Effect of flow rate (L/h) of the fluid

The SEM images of the particles obtained at the 6th stage at different flow rates are shown in Fig. 9. From these images, microparticles were detected by increasing the flow rate. The particle size observed at flow rate 0.2 L/h is 25–33 nm (Fig. 9a), at flow rate 0.3 L/h is 0.11–0.59 μm (Fig. 9b) and at flow rate 0.4 L/h is 0.8–8.6 μm (Fig. 9c).

To illustrate the particle size diversity at different flow rates Eq. 6 is consulted, and

$$\mu = \text{F.R} / L \quad (9)$$

where F.R: flow rate and L: vertical travelled distance. Therefore,

$$d^2 = (18v_s/g) * [1/L(\rho_s - \rho_f)] * \text{F.R} \quad (10)$$

For certain concentration and at 6th stage, the term $[1/L(\rho_s - \rho_f)]$ is constant and for certain particle v_s is constant. Therefore,

$$d^2 = k_3 * \text{F.R} \quad (11)$$

The d^2 was plotted vs. FR, the relation traced in Fig. 10, shows clearly that as the flow rate increases, the particle size increases linearly with the slope around 1.4×10^{-3} m s kg^{-1} which support Eq. 11.

The best conditions of the above factors are [$CaCO_3$ weight (5 g), 0.8 L water, stirring speed (650 rpm), stirring

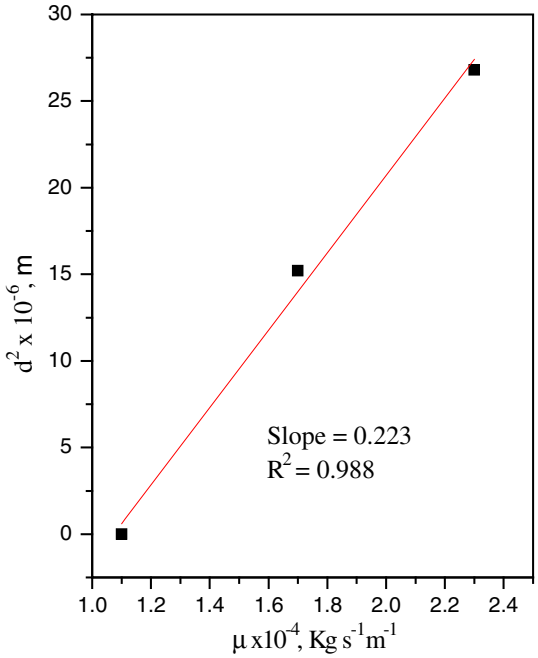

Fig. 8 Effect of dynamic viscosity of fluid particle size of $CaCO_3$ obtained at 6th stage

time (2 h), flow rate (0.2 L/h), and 6th stage] were applied on $CaCO_3$ of sample S2. Figure 11 shows the particles obtained with size ranged between 25 and 48 nm.

Characterization of calcium carbonate

XRD analysis

X-ray diffraction patterns for the two samples S1 and S2 before and after fractionation are given in Figs. 12 and 13, respectively. From the figures, an intense sharp peak at $2\theta = 29°$ is obtained for both samples before and after fractionation. This indicates that $CaCO_3$ have crystal structure, this crystalline polymorph is calcite. The crystal size obtained for S1 (Fig. 12) are $D = 55$ nm and $D = 42$ nm before and after fractionation, respectively. In addition, the crystal sizes obtained for S2 (Fig. 13) are $D = 48$ nm and $D = 42$ nm before and after fractionation, respectively. The crystal size was calculated using Scherrer's equation. These values are comparable with that obtained by SEM; however, SEM

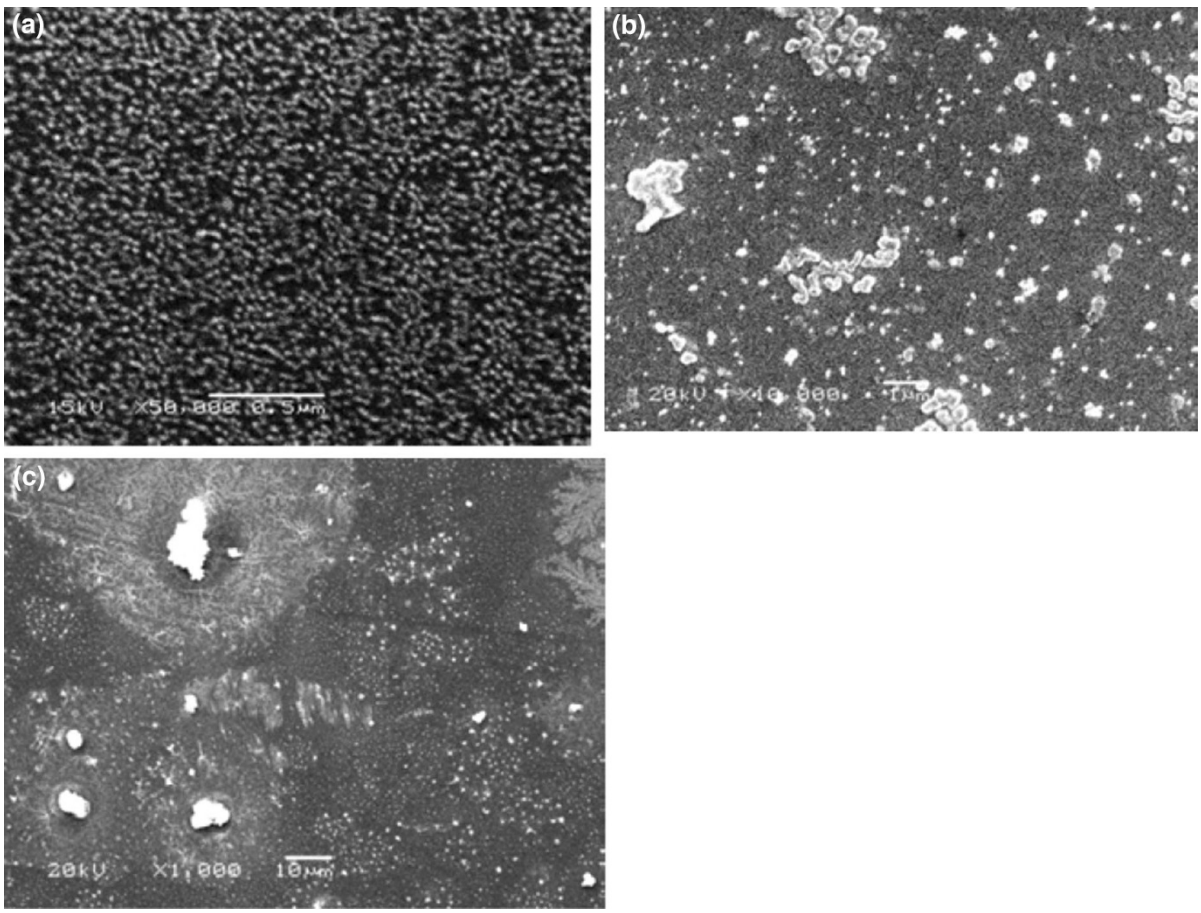

Fig. 9 Effect of flow rate (L/h) of the fluid. 6th stage, Stirring time: 2 h. Stirrer speed: 650 rpm. [$CaCO_3$]: 5 g/800 L. F.R. **a** 0.2 L/h, **b** 0.3 L/h and **c** 0.4 L/h

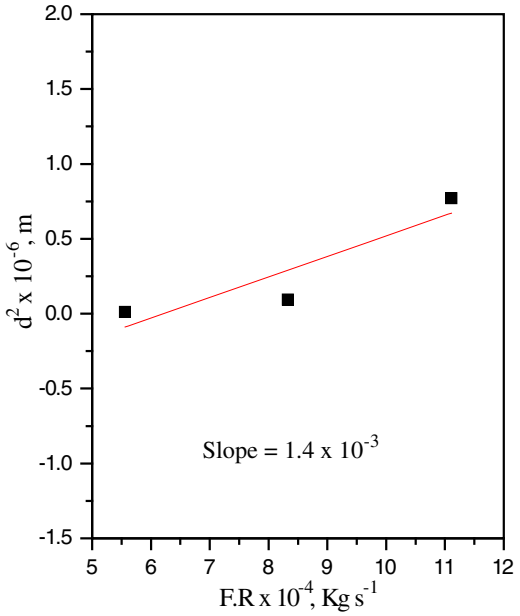

Fig. 10 Effect of flow rate on the $CaCO_3$ particle size at 6th stage

results are more detailed concerning the particle size distribution if statistically examined carefully.

FTIR analysis

The IR spectra of $CaCO_3$ nanoparticles fractionated from S1 and S2, respectively, (a: before fractionation and b: after fractionation for each samples) are given in Figs. 14 and 15. $CaCO_3$ has three main peaks $v_3 = 1{,}425\ cm^{-1}$, $v_2 = 874\ cm^{-1}$ and $v_4 = 712\ cm^{-1}$ (Yue Lin-hai et al. 2000). The v_3 band is strong and broad while v_2 and v_4 bands are weak and narrow. The main peaks in our samples (S1 and S2) are shown at $v_3 = 1{,}465\ cm^{-1}$ (strong and broad band), $v_2 = 868\ cm^{-1}$ (weak and broad band) and $v_4 = 663\ cm^{-1}$ (weak and broad band). Furthermore, for S1, the band at $1{,}465\ cm^{-1}$ obtained before fractionation, Fig. 14a, is more broader than that obtained after fractionation, Fig. 14b. And the band at $3{,}444\ cm^{-1}$ related to the O–H vibrational mode for the adsorbed water obtained before fractionation, Fig. 14a, is less intense than that obtained after fractionation, Fig. 14a. This may be

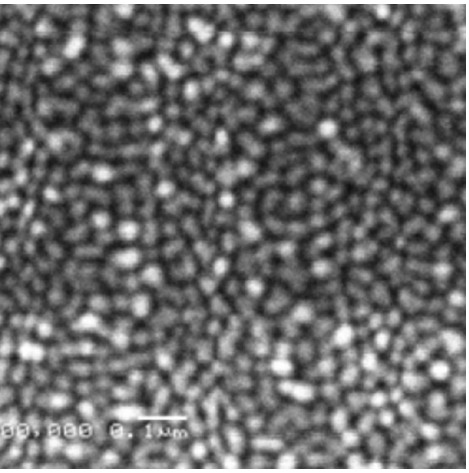

Fig. 11 Image of particles obtained from $CaCO_3$ from Riedel-deHaën (S2). [$CaCO_3$]: 5 g/800 L. Stirring speed: 650 rpm. Stirring time: 2 h, Flow rate: 0.2 L/h. 6th stage, water volume: 0.80 L

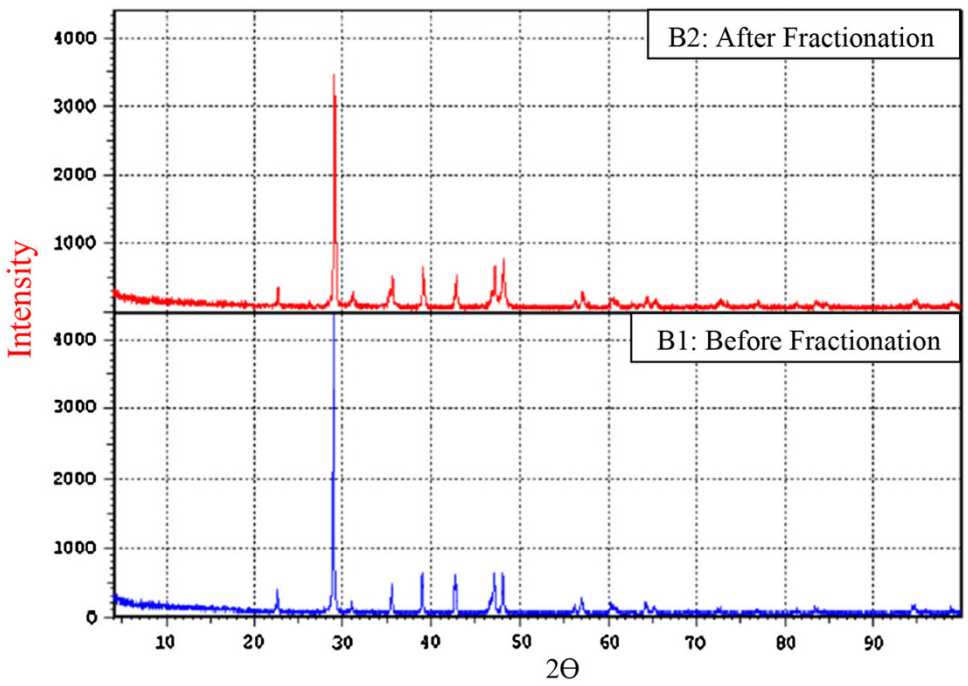

Fig. 12 XRD characterization peaks for $CaCO_3$ from Target for chemical industry company (S1); B1: before ($D = 55$ nm) and B2: after fractionation ($D = 42$ nm)

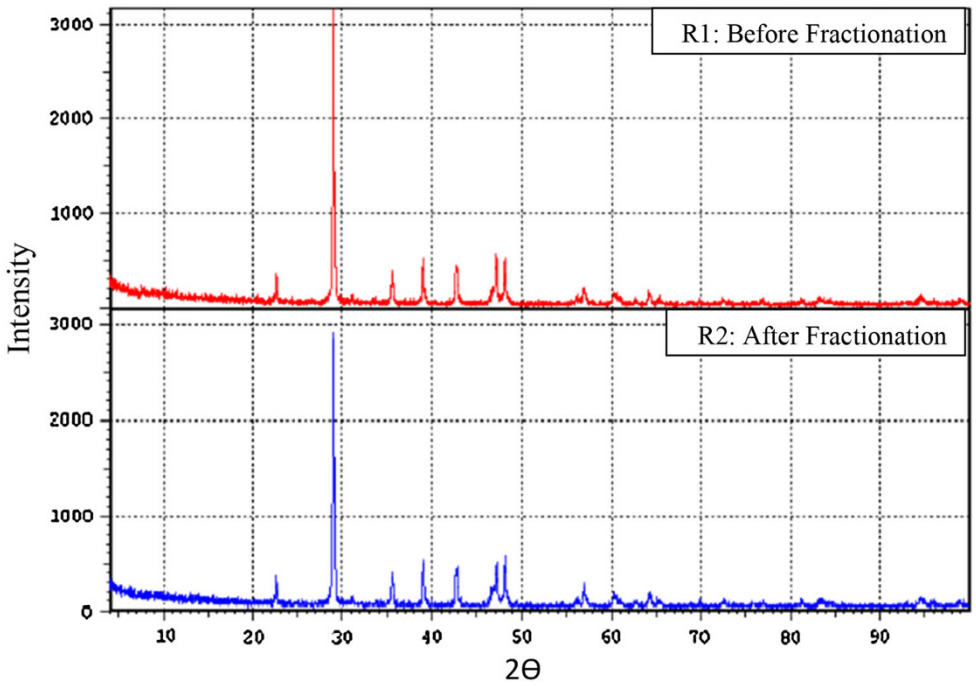

Fig. 13 XRD characterization peaks for $CaCO_3$ from Riedel-deHaën (S2); R1: before($D = 48$ nm) and R: after fractionation ($D = 42$ nm)

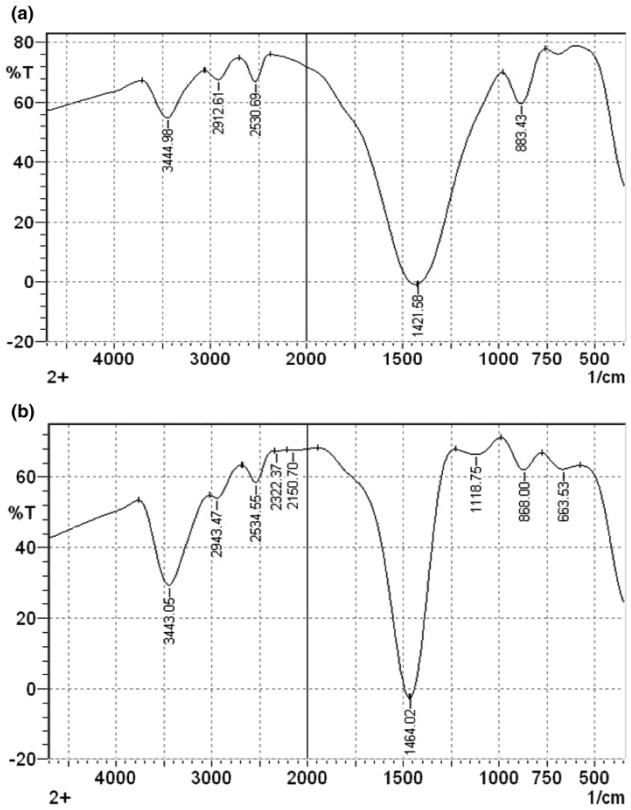

Fig. 14 FTIR spectrum of fractionated $CaCO_3$ nanoparticles from S1: **a** before and **b** after fractionation

referring to the high reactivity of the fractionated $CaCO_3$ nanoparticles. Similarly, for S2 the band at 3,444 cm^{-1} related to the O–H vibrational mode for the adsorbed water obtained before fractionation, Fig. 15a, is less intense than that obtained after fractionation, Fig. 15b.

EDS of fractionated $CaCO_3$ nanoparticles

Figures 16 and 17 revealed to the EDS analysis for the $CaCO_3$ nanoparticles obtained after fractionation form the two samples S1 and S2, respectively. The two figures showed that the $CaCO_3$ nanoparticles obtained have some impurities. By comparison between the EDS analysis for the sample S1 (before; Fig. 3 and after; Fig. 16), we observed that some impurities disappear and another impurities decrease to very low percent. The purity of the sample S2 increases from 98.5 to 99.77 %.

Conclusion

In this work, we developed a laboratory scale hydraulic classifier system for fractionation of calcium carbonate nanoparticles. The used procedure is very simple and relatively of low cost where water was used as fractionation medium, a feeding pump and simple glassware. By this system, we fractionate calcium carbonate of commercial resources to particle diameters in the range 25–33 nm and 25–48 nm by varying the different parameters. The experimental results were modeled in terms of the different parameters affecting particles fractionations.

Although the developed system is simple and easy to manufacture, yet the time required for fractionation is

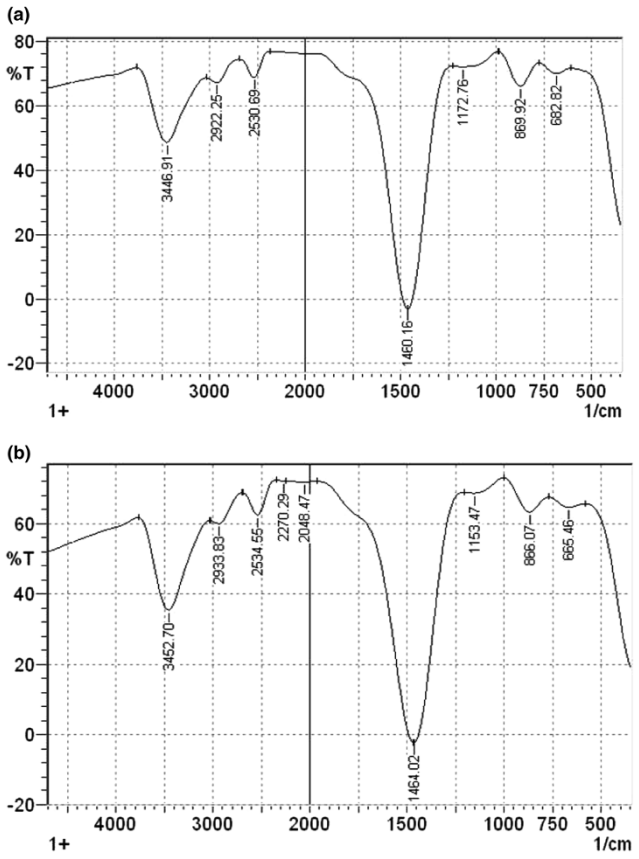

Fig. 15 FTIR spectrum of fractionated $CaCO_3$ nanoparticles from S2: **a** before and **b** after fractionation

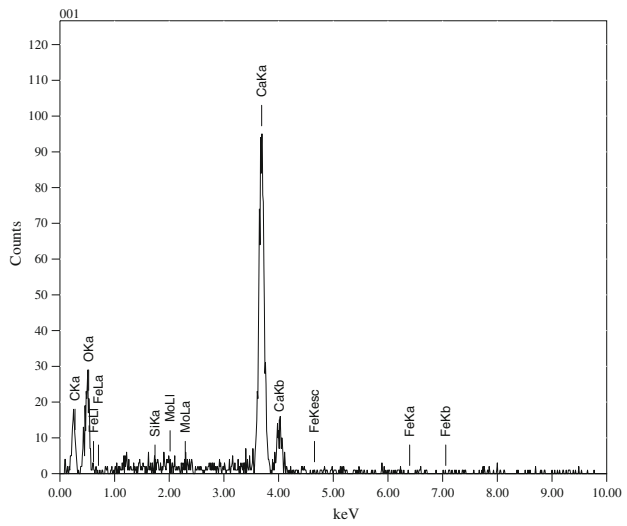

Element	(keV)	mass%	Error%	At%	Compound	mass%	Cation K
C K	0.277	11.18	0.15	19.26			7.1719
O K	0.525	45.42	0.90	58.73			19.9788
Si K	1.739	0.18	0.20	0.13			0.2079
Ca K	3.690	41.80	0.26	21.57			70.7815
Mo L	2.293	1.43	0.47	0.31			1.8599
Total		100.00		100.00			

Fig. 16 The EDS analysis for calcium carbonate obtained from Riedel–DeHaen Company (S1) after fractionation

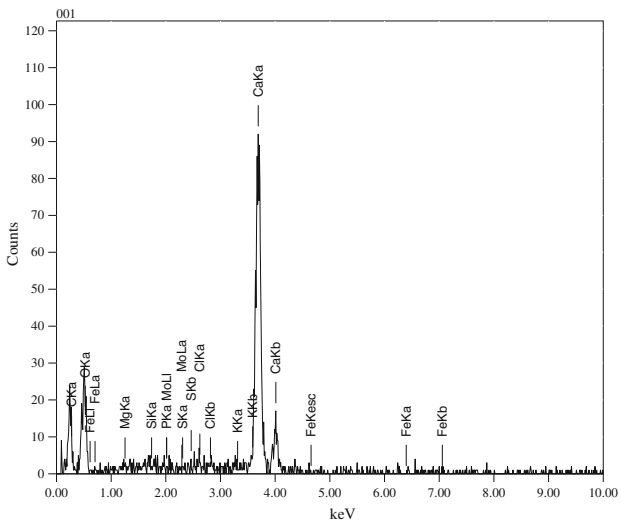

Element	(keV)	mass%	Error%	At%	Compound	mass%	Cation K
C K	0.277	7.76	0.16	13.38			4.9740
O K	0.525	49.98	0.93	64.73			23.3164
S K	2.307	0.04	0.16	0.03			0.0680
Cl K	2.621	0.34	0.18	0.20			0.5614
Ca K	3.690	41.88	0.28	21.66			71.0802
Total		100.00		100.00			

Fig. 17 The EDS analysis for calcium carbonate obtained from Riedel–DeHaen Company (S2) after fractionation

relatively long compared to density gradient centrifugation. However, the density gradient centrifugation requires a suitable centrifuge and density gradient medium which do not disturb the nanoparticles to be separated further is needs more expensive components.

From the characterization of the fractionated nanoparticles from the two samples S1 and S2, the nanoparticles more reactive, have small crystal size and high purity compared by the original samples used.

Open Access This article is distributed under the terms of the Creative Commons Attribution License which permits any use, distribution, and reproduction in any medium, provided the original author(s) and the source are credited.

References

Barry AW, Napier-Munn T (2006) An introduction to the practical aspects of ore treatment and mineral recovery. Elsevier Science & Technology Books, l7th edition

Bryczkowski A, Chmielniak T (2001) Method of calculation of new cyclone-type separator with swirling baffle and bottom take off of clean gas—part II: experimental verification. Chem Eng Process 40:245–254

Galk J, Peukert W, Krahnen J (1999) Industrial classification in a new impeller wheel classifier. Powder Technol 105:186–189

Guo Feng, Li Ying, Hong-Xia Xu, Zhao Guo-Qing, He Xiu-Juan (2007) Size-controllable synthesis of calcium carbonate nanoparticles using aqueous foam films as templates. Mater Lett 61:4937–4939

Kowalczyk Bartlomiej, IstvanLagzi, Grzybowski BA (2011) Nanoseparations: strategies for size and/or shape-selective purification of nanoparticles. Curr Opin Colloid Interface Sci 16:135–148

Lin-hai Yue, Shui Miao Xu, Zhu-de Xu X (2000) Distortion of crystal lattice and abnormal infra-red behavior in nanocrystalline $CaCO_3$. J Zhejiang Univ (SCIENCE) 1:178–183

Rhods M (2008) Introduction to particle technology Handbok, 2nd edn. Wiley, New York

Stokes GG (1891) Mathematical and physical paper III. Cambridge University Press, Cambridge

Sun XM, Tabakman SM, Seo WS et al (2009) Separation of nanoparticles in a density gradient: FeCo@C and gold nanocrystals. Ange Chem Int Ed 48:939–942

Van Kooy L, Mooij M, Rem P (2004) Kinetic gravity separation. Phys Sep Sci Eng 13:25–32

Vigneau E, Loisel C, Devaux MF, Cantoni P (2000) Number of particles for the determination of size distribution from microscopic image. Powder Technol 107:243–250

Wang Q, Chr Melaaen M, De Silva SR (2001) Investigation and simulation of a cross-flow air classifier. Powder Technol 120:273–280

www.gordonengland.co.uk/conversion/dynamic_viscosity.htm

Yamamoto Ken-ichi, Tohyama Masakazu, Sugimoto Masunori (1998) Continuous separation of differently shaped fine particles on a rotating vibrating conical disk effects of different operating conditions on separation characteristics under various throughputs. Powder Technol 99:1–10